

# Metallaindenes of Molybdenum, Tungsten, and Ruthenium

Jing Yang, Jianguo Yin, Khalil A. Abboud, and W. M. Jones\*

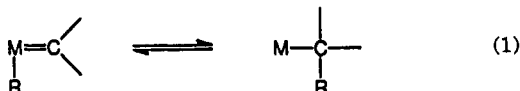
Department of Chemistry, University of Florida, Gainesville, Florida 32611

Received October 13, 1993\*

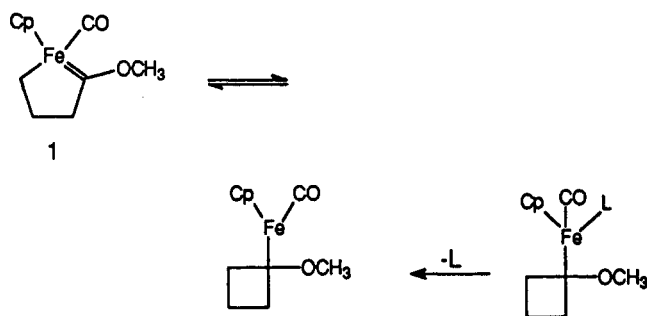
Five metallaindene complexes of molybdenum, tungsten, and ruthenium [3a (Mo), 3b (W), 3c (Ru), 5a (Ru), and 5b (Ru)] have been prepared. The complexes of molybdenum and tungsten show fluxional behavior for which a pseudorotation mechanism is suggested. Reaction of the ruthenium complex 3c with phenyllithium or *p*-tolyllithium followed by CF<sub>3</sub>SO<sub>2</sub>OSiMe<sub>3</sub> gives aryl substituted ruthenaindenes 5a and 5b. In solution, these complexes quantitatively rearrange to form ruthenocene derivatives 11a and 11b. A mechanism for this rearrangement which includes a series of carbonyl and carbene insertions is proposed. Crystallographic data for 3b:  $P2_1/n$ ,  $a = 9.945(2)$  Å,  $b = 13.207(2)$  Å,  $c = 11.304(2)$  Å,  $\alpha = 90^\circ$ ,  $\beta = 107.38(2)^\circ$ ,  $\gamma = 90^\circ$ ,  $Z = 4$ . For 5a:  $P2_1/n$ ,  $a = 9.082(1)$  Å,  $b = 10.601(1)$  Å,  $c = 16.827(2)$  Å,  $\alpha = 90^\circ$ ,  $\beta = 92.57(1)^\circ$ ,  $\gamma = 90^\circ$ ,  $Z = 4$ . For 11b:  $P2_12_12_1$ ,  $a = 8.452(1)$  Å,  $b = 12.558(1)$  Å,  $c = 15.812(2)$  Å,  $\alpha = \beta = \gamma = 90^\circ$ ,  $Z = 4$ .

## Introduction

Stable Fischer carbene complexes of first and second row transition metals substituted with alkyl or aryl ligands are rare due to a profound tendency of the alkyl or aryl group to rearrange to the carbene carbon in a reaction that is commonly referred to as a carbene migratory insertion reaction (eq 1, left to right).<sup>1-5</sup> However, we have



found not only that incorporation of the carbene into a five membered ring in which migratory insertion is retarded by ring strain permits the isolation of such complexes<sup>4-6</sup> but also that strain relief during the reverse reaction ( $\alpha$ -elimination) has provided a convenient way to prepare metallacyclopentenes (e.g. 1) and metallaindenes of both iron and manganese<sup>4-6</sup> complexes that were



desirable for the study of the carbene migratory insertion reaction.<sup>4</sup> Unfortunately, this methodology failed when applied to the second and third row metals, ruthenium, rhenium, or tungsten.<sup>4c,7</sup> In a recent communication<sup>4c</sup> we reported an approach to metallacyclopentenes<sup>8</sup> which was successfully applied to the preparation of a ruthenacyclopentene and the corresponding ferracyclopentene. At this time we report the application of this synthetic methodology to the preparation of metallaindenes of ruthenium, molybdenum, and tungsten and a novel thermal rearrangement of the ruthenium complex.

## Results and Discussion

(2-Bromobenzyl)metal  $\sigma$  complexes 2 were readily prepared (Scheme 1) in moderate to high yield by reaction of 2-bromobenzyl bromide with the appropriate anion. Treatment of these  $\sigma$  complexes with stoichiometric amounts of *n*-BuLi in THF at  $-100^\circ\text{C}$  followed by warming to room temperature overnight and treatment with Me<sub>3</sub>OBf<sub>4</sub> gave red crystals of 3 in moderate yield.

Complexes 3 were characterized by <sup>1</sup>H and <sup>13</sup>C NMR, IR, and elemental analyses. All are moderately air sensitive and, to our knowledge, are the first examples of metal-

(7) Unpublished results of P. Hanna and D. J. Crowther, University of Florida.

(8) This synthetic method is similar to that applied by Allison for the preparation of metallabenzenes. See: (a) Ferede, R.; Allison, N. T. *Organometallics* 1983, 2, 463. (b) Ferede, R.; Hinton, J. F.; Korfmacher, W. A.; Freeman, J. P. *Organometallics* 1985, 4, 614. (c) Mike, C. A.; Ferede, R.; Allison, N. T. *Organometallics* 1988, 7, 1457.

\* Abstract published in *Advance ACS Abstracts*, February 1, 1994.

(1) Both "carbene migratory insertion" and "carbonyl insertion" are terms that are so widely used<sup>2</sup> that we shall continue this custom although the reader should be aware that it is highly unlikely that either accurately connotes the actual movement of atoms.

(2) Cf.: Collman, J. P.; Hegedus, L. S.; Norton, J. R.; Finke, R. G. *Principles and Applications of Organotransition Metal Chemistry*; University Science Books: Mill Valley, CA, 1987.

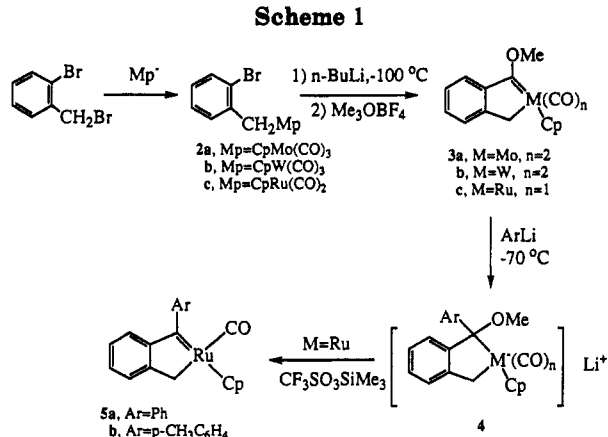
(3) (a) Threlkel, R. S.; Bercaw, J. W. *J. Am. Chem. Soc.* 1981, 103, 2650. (b) Thorn, D. L.; Tulip, T. H. *J. Am. Chem. Soc.* 1981, 103, 5984. (c) Barger, P. T.; Bercaw, J. E. *Organometallics* 1984, 3, 278. (d) Thorn, D. L. *Organometallics* 1985, 4, 192. (e) Fryzuk, M. D.; MacNeil, P. A.; Rettig, S. J. *J. Am. Chem. Soc.* 1985, 107, 6708. (f) Jerknakoff, P.; Cooper, N. N. *Organometallics* 1986, 5, 747. (g) Jones, W. D.; Kosar, W. P. *J. Am. Chem. Soc.* 1986, 108, 5640. (h) Carter, E. A.; Goddard, W. A., III. *Organometallics*, 1988, 7, 675. (i) Cantrell, R. D.; Shevlin, P. B. *J. Am. Chem. Soc.*, 1989, 111, 2349. (j) O'Connor, J. M.; Pu, L.; Rheingold, A. L. *J. Am. Chem. Soc.* 1989, 111, 4129. (k) Hughes, R. P.; Trujillo, H. A.; Rheingold, R. L. *J. Am. Chem. Soc.* 1993, 115, 1583.

(4) (a) Stenstrom, Y.; Jones, W. M. *Organometallics* 1986, 5, 178. (b) Stenstrom, Y.; Koziol, P.; Palenik, G. J.; Jones, W. M. *Organometallics* 1987, 6, 2079. (c) Trace, R. L.; Sanchez, J.; Yang, J.; Yin, J.; Jones, W. M. *Organometallics* 1992, 11, 1440.

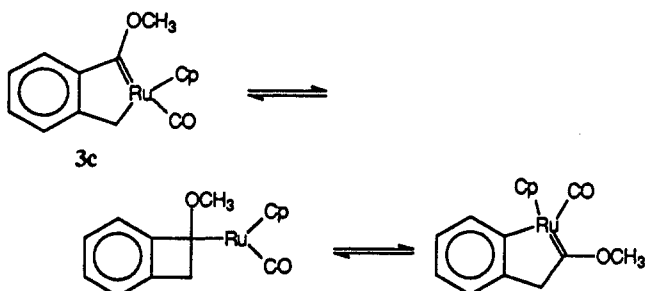
(5) Conti, N. J.; Jones, W. M. *Organometallics* 1988, 7, 1666-1669.

(6) (a) Conti, N. J.; Crowther, D. J.; Tivakornpannarai, S.; Jones, W. M. *Organometallics* 1990, 9, 175-184. (b) Crowther, D. J.; Tivakornpannarai, S.; Jones, W. M. *Organometallics* 1990, 9, 739. (c) Crowther, D. J.; Zhang, Z.; Palenik, G. J.; Jones, W. M. *Organometallics* 1992, 11, 622.

## Scheme 1



indenyl complexes of second or third row transition metals. As with their first row analogues,<sup>6b,9</sup> 3a–c are all



thermally stable, showing no evidence of carbene migratory insertion (which could be readily detected by their rearrangement to isomeric metallaindenes). For example, 3c showed no change after heating at 80 °C for 5 days or photolysis in the presence of PMe<sub>3</sub> for 6 h.

The <sup>1</sup>H NMR spectra of 3 showed pairs of doublets around 2.7–3.2 ppm that are characteristic of diastereotopic hydrogens. However, while the ruthenium doublets were insensitive to temperature change, those of molybdenum and tungsten showed coalescence upon warming (for 3a, 105 °C in C<sub>7</sub>D<sub>8</sub>; for 3b, 41, 48, and 52 °C in C<sub>6</sub>D<sub>12</sub>, CDCl<sub>3</sub>, and CD<sub>3</sub>CN, respectively). To explain the coalescence, we suggest the pseudorotation mechanism depicted in Figure 1. For this process we begin with a, the structure confirmed in the crystal X-ray diffraction. Pseudorotation from a to d via b and c gives a structure with the symmetry required to make the diastereotopic hydrogens equivalent. Finally, a is regenerated via e and f (or b and c). Interestingly, in aromatic solvents (benzene and toluene) the two diastereotopic hydrogens of 3b appear as a singlet, even well below 0 °C. This suggested either a profound solvent effect on the fluxionality or a solvent effect that simply led to an accidental degeneracy of the two diastereotopic hydrogens. That it is the latter was confirmed in three ways. First, <sup>13</sup>CO enriched 3b was prepared from W(CO)<sub>4</sub>(<sup>13</sup>CO)<sub>2</sub>. If the singlet in the proton spectrum were the result of rapid formation of d, only one terminal carbonyl should be observed in the <sup>13</sup>C NMR at room temperature. In fact, in C<sub>7</sub>D<sub>8</sub> two terminal CO resonances were clearly seen. Upon warming to about 70 °C, these resonances disappeared into the baseline to reappear as a broad singlet at about 90 °C (at higher temperatures decomposition occurred during the long acquisition times required). Despite the enrichment, the CO signals were

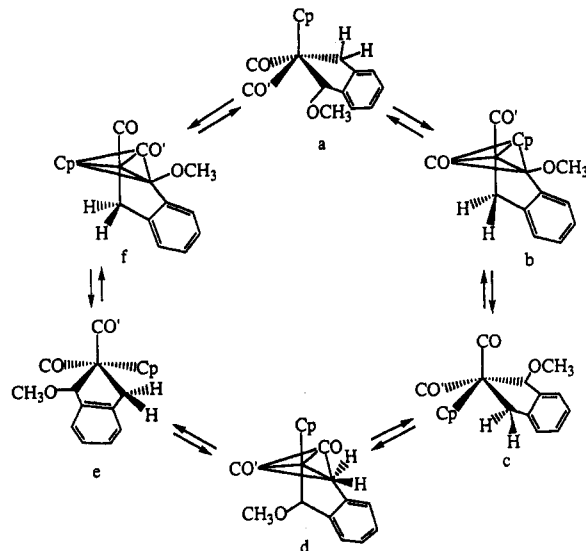


Figure 1. Pseudorotation of 3a and 3b showing equivalency of the methylene hydrogens and carbonyls in structure d.

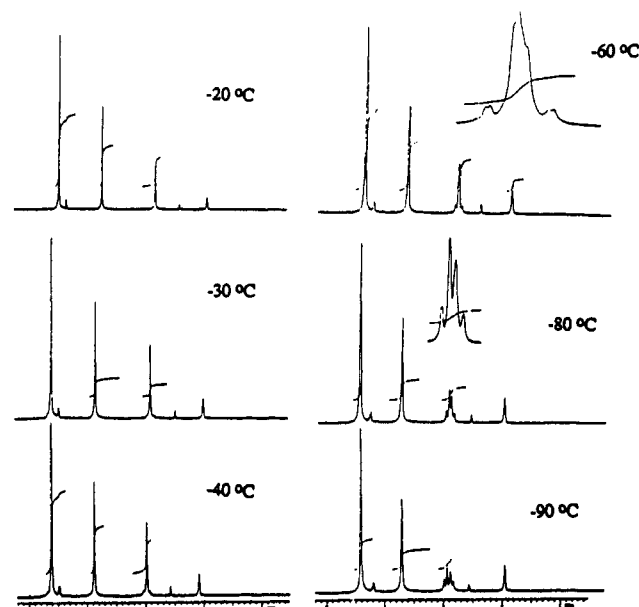


Figure 2. Temperature dependent <sup>1</sup>H NMR spectrum of 3b highlighting CH<sub>2</sub> resonances.

too weak to permit determination of an accurate coalescence temperature. However, these two temperatures place the barrier to fluxionality ( $\Delta G^\ddagger$ ) between 15.2 and 16.1 kcal/mol, which bracket the  $\Delta G^\ddagger$  (15.6 kcal/mol; 1:1 C<sub>7</sub>D<sub>8</sub>:CDCl<sub>3</sub>) that was determined from coalescence of the AB pattern of the diastereotopic hydrogens at 38 °C ( $\Delta\nu = 36$  Hz) in the <sup>1</sup>H NMR. Second, although the chemical shifts of the two diastereotopic hydrogens in 3b are temperature dependent at very low temperatures in the aromatic solvent C<sub>7</sub>D<sub>8</sub>, this dependence is not consistent with fluxionality. Thus, the pair of doublets (Figure 2) at  $\delta$  2.94 and 3.06 ppm that appear at -90 °C, do indeed coalesce into a single sharp peak at -20 °C but the changes are not typical of coalescence of an AB pattern that results from fluxionality and instead are consistent with changes expected of an AB pattern when the chemical shift difference decreases relative to the coupling constant.<sup>10</sup>

(9) Stenstrom, Y.; Klauk, G.; Koziol, A.; Palenik, G. J.; Jones, W. M. *Organometallics* 1986, 5, 2155.

(10) Sandström, J. *Dynamic NMR Spectroscopy*; Academic Press: New York, 1982.

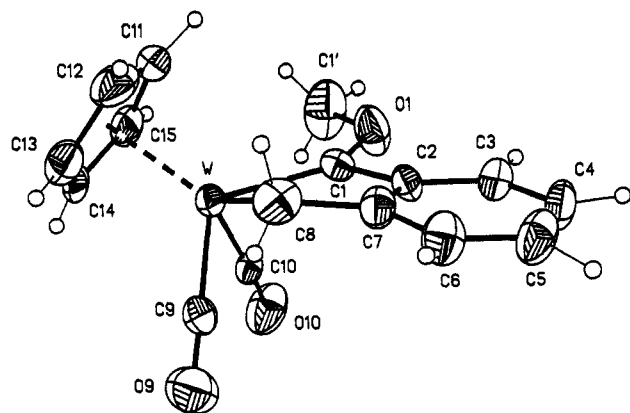


Figure 3. Structure and labeling scheme for **3b** with 50% probability thermal ellipsoids.

Table 1. Fractional Coordinates and Equivalent Isotropic Thermal Parameters ( $\text{\AA}^2$ ) for the Non-H Atoms of Compound **3b**

atom	x	y	z	U
W	0.14953(4)	0.14650(3)	0.35257(3)	0.03588(12)
O1	-0.0251(8)	-0.0230(6)	0.1756(9)	0.074(3)
O9	0.0896(10)	0.3795(6)	0.3205(9)	0.078(4)
C1	-0.0199(10)	0.0602(7)	0.2445(8)	0.043(3)
C1'	0.1025(14)	-0.0711(11)	0.1684(14)	0.091(6)
C2	-0.1658(9)	0.0911(7)	0.2293(8)	0.041(3)
C3	-0.2858(11)	0.0542(10)	0.1405(10)	0.056(4)
C4	-0.4146(11)	0.0965(10)	0.1352(11)	0.063(4)
C5	-0.4240(12)	0.1742(11)	0.2135(11)	0.067(5)
C6	-0.3072(12)	0.2074(12)	0.3022(12)	0.059(5)
C7	-0.1777(10)	0.1644(8)	0.3142(8)	0.046(3)
C8	-0.0453(11)	0.1904(9)	0.4092(9)	0.057(4)
C9	0.1113(10)	0.2917(8)	0.3320(9)	0.045(3)
C10	0.1594(9)	0.1639(7)	0.1854(9)	0.043(3)
C11	0.2689(13)	0.0080(10)	0.4740(13)	0.069(5)
C12	0.2531(14)	0.0845(12)	0.5567(11)	0.072(6)
C13	0.3275(13)	0.1712(10)	0.5426(10)	0.060(4)
C14	0.3895(10)	0.1487(9)	0.4500(9)	0.051(3)
C15	0.3568(11)	0.0494(9)	0.4087(10)	0.057(4)

<sup>a</sup> For anisotropic atoms, the  $U$  value is  $U_{\text{eq}}$ , calculated as  $U_{\text{eq}} = 1/3 \sum_i \sum_j U_{ij} a_i^* a_j^* A_{ij}$  where  $A_{ij}$  is the dot product of the  $i$ th and  $j$ th direct space unit cell vectors.

We have no explanation for the fact that this peak remains as a singlet as the temperature is raised further (to 105 °C). Finally, as mentioned above, the presence of the aromatic solvent in a mixture of  $\text{CDCl}_3$  and  $\text{C}_7\text{D}_8$  (1:1, v/v) failed to cause a large solvent effect on the fluxionality barrier ( $T_c = 38$  °C,  $\Delta G^\ddagger = 15.6$  kcal/mol; in pure  $\text{CDCl}_3$   $T_c = 48$  °C,  $\Delta G^\ddagger = 15.1$  kcal/mol). The higher coalescence temperature for the molybdenum complex is presumably steric in origin due to shorter metal-carbon bonds.

The structure of **3b** was confirmed by X-ray analysis. An ORTEP plot is shown in Figure 3, the positional parameters are collected in Table 1, and selected bond distances and angles are listed in Table 2. The molecule has pseudo-square pyramidal geometry with bond distances for W—C1 and W—C8 of 2.098(9) and 2.289(12) Å, respectively, as would be expected of typical metal-carbon single and double bonds.<sup>11</sup> The bond distance for C1—O1 is 1.338(13) Å, which is about as expected of an  $\text{sp}^2$ -O bond in which the oxygen donates electrons to an electron deficient  $\pi$ -system.<sup>12</sup> The plane defined by W, C1, and C8 forms an angle of 160.4(3)° with the phenyl ring. This

Table 2. Selected Bond Lengths (Å) and Angles (deg) for **3b**

Bond Lengths			
W—C1	2.098(9)	W—C8	2.289(12)
W—C9	1.955(11)	W—C10	1.935(10)
W—C11	2.381(13)	W—C12	2.374(12)
W—C13	2.362(10)	W—C14	2.311(9)
W—C15	2.348(11)	C1—O1	1.338(13)
C1'—O1	1.44(2)	C9—O9	1.179(14)
C10—O10	1.171(14)	C1—C2	1.468(14)
C2—C3	1.398(12)	C2—C7	1.391(14)
C8—C7	1.470(13)		
Bond Angles			
C1—W—C8	72.6(4)	C1—W—C9	111.7(3)
C1—W—C10	76.2(4)	C8—W—C9	68.5(4)
C8—W—C10	122.5(4)	C9—W—C10	80.3(4)
C1—O1—C1'	120.8(8)	C2—C1—W	120.7(7)
C2—C1—O1	107.2(7)	C7—C2—C1	113.4(7)
C8—C7—C2	115.1(9)	C8—C7—C6	125.6(10)
W—C8—C7	112.6(8)	W—C9—O9	179.3(8)
W—C10—O10	175.7(8)		

bending, also reflected by the torsion angle described by W—C1—C2—C7 [ $-15(1)^\circ$ ], is indicative of reduced conjugation between the W=C1 double bond and the phenyl ring.

Carbene migratory insertion in **3** is retarded by both ring strain in the resulting benzocyclobutene (46.9 kcal/mol from MMX calculations<sup>13</sup>) and methoxy stabilization of the carbene that is lost upon rearrangement. With an eye to observing migratory insertion in these complexes, attempts were made to replace the methoxy substituent<sup>14</sup> with the poorer electron donating phenyl group.<sup>15</sup> These attempts failed for **3a** and **3b**. Although treatment of either with a slight excess of ArLi (Ar = Ph, *p*-tolyl) in THF gave brown adducts, presumably salts **4** (Scheme 1), no metal containing products could be isolated from their reaction with such methoxy abstracting agents as  $\text{CF}_3\text{SO}_3\text{SiMe}_3$ ,  $\text{CF}_3\text{COOH}$ ,<sup>16</sup> and  $\text{SiO}_2$ .<sup>17</sup> However, it was found that the brown adducts from the reaction of **4c** with a slight excess of phenyllithium or *p*-tolyllithium with  $\text{CF}_3\text{SO}_3\text{SiMe}_3$  at a low temperature gave **5a** and **5b** as air-sensitive black crystals in moderate yield (Scheme 2).

Complexes **5a** and **5b** are, to the best of our knowledge, the first examples of stable alkyl substituted Fischer carbene complexes of ruthenium without a heteroatom stabilizing substituent on the carbene carbon. Both showed terminal CO absorptions at 1968 and 1966  $\text{cm}^{-1}$ , respectively, and characteristic carbene-carbon resonances in the  $^{13}\text{C}$  NMR at  $\delta$  309.5 and 309.2 ppm for **5a** and **5b**, respectively. These are at a somewhat lower field than the carbene resonance of **3c** (294.2 ppm) which is consistent with somewhat reduced electron density on the carbene carbon in the aryl substituted molecules, not only because the phenyl is inherently a poorer electron donor than methoxy<sup>15</sup> but also, at least in the crystal, because the phenyl is out of conjugation with the carbon-metal double bond.

The molecular structure of **5a** as determined by X-ray crystallography is shown in Figure 4; selected bond lengths

(13) MMX program generously provided by Professor J. J. Gajewski, Department of Chemistry, Indiana University.

(14) Cf.: Dotz, K. H.; Fischer, H.; Hofmann, P.; Kreissl, F. R.; Schubert, U.; Weiss, K. *Transition Metal Carbene Complexes*; Verlag Chemie: Weinheim, 1983.

(15) Reference 12, p 280.

(16) Casey, C. P.; Albin, L. D.; Burkhardt, T. J. *J. Am. Chem. Soc.* 1977, 99, 2533.

(17) Fischer, E. O.; Held, W.; Kreisl, F. R.; Frank, A.; Huttner, G. *Chem. Ber.* 1977, 110, 656.

(11) Stone, F. G. A.; Robert, W. *Adv. Organomet. Chem.* 1976, 14, 1.  
 (12) March, J. *Advanced Organic Chemistry*, 4th ed.; Wiley: New York, 1992; p 21.

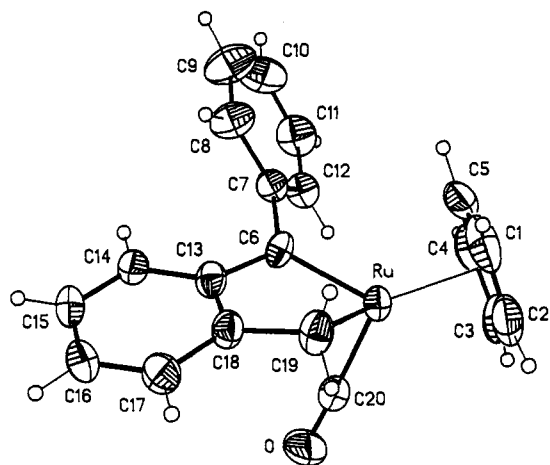


Figure 4. Structure and labeling scheme for 5a with 50% probability thermal ellipsoids.

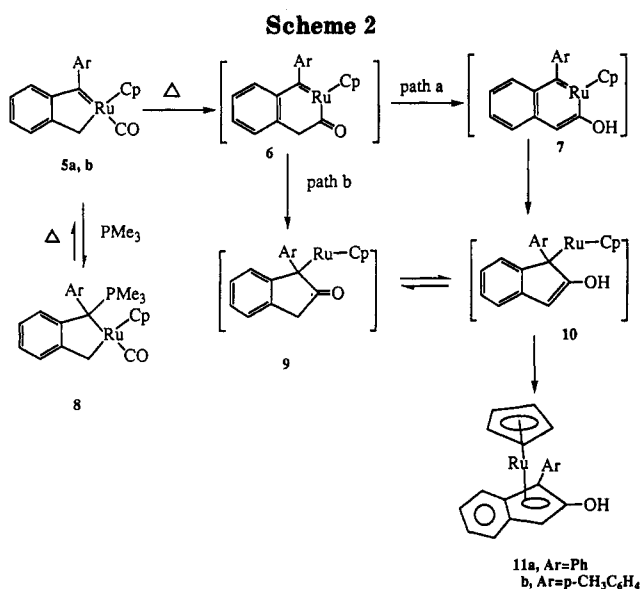


Table 3. Selected Bond Lengths (Å) and Angles (deg) for 5a

Bond Lengths			
Ru-C(1)	2.246(7)	Ru-C(2)	2.260(7)
Ru-C(3)	2.286(7)	Ru-C(4)	2.289(6)
Ru-C(5)	2.277(7)	Ru-C(6)	1.949(5)
Ru-C(19)	2.135(6)	Ru-C(20)	1.834(6)
C(20)-O	1.152(8)	C(1)-C(2)	1.398(14)
C(2)-C(3)	1.401(12)	C(3)-C(4)	1.390(12)
C(4)-C(5)	1.378(12)	C(1)-C(5)	1.413(12)
C(6)-C(7)	1.470(7)	C(6)-C(13)	1.444(7)
C(13)-C(14)	1.411(8)	C(13)-C(18)	1.404(7)
C(14)-C(15)	1.384(8)	C(15)-C(16)	1.383(10)
C(16)-C(17)	1.379(9)	C(17)-C(18)	1.396(8)
C(18)-C(19)	1.482(8)		
Bond Angles			
C(6)-Ru-C(19)	79.0(2)	C(19)-Ru-C(20)	84.1(3)
C(7)-C(6)-C(13)	119.8(4)	C(13)-C(6)-Ru	115.9(3)
C(6)-C(13)-C(14)	127.0(5)	C(6)-C(13)-C(18)	113.9(5)
C(13)-C(18)-C(19)	114.1(5)	C(17)-C(18)-C(19)	126.3(5)
Ru-C(19)-C(18)	107.5(4)		

and angles are given in Table 3 and atomic parameters are given in Table 4. The compound has a pseudooctahedral geometry with the Cp ring on the top. The bond distance between C6 (carbene carbon) and Ru is 1.949(5) Å, a typical bond length for a metal-carbon double bond.<sup>11</sup> Only one phenyl ring (benzo ring) was found to be conjugated with the Ru-carbene bond. As a result, the C6-C13 bond length of 1.444(7) Å is shorter than C6-C7 [1.470(7) Å], which is

Table 4. Fractional Coordinates and Equivalent Isotropic Thermal Parameters (Å<sup>2</sup>) for the Non-H Atoms of Compound 5

atom	x	y	z	U
Ru	0.24506(5)	0.06450(4)	0.10132(2)	0.04017(14)
O	-0.0043(5)	-0.1035(5)	0.1420(3)	0.078(2)
C1	0.3202(11)	0.2295(6)	0.0299(5)	0.075(4)
C2	0.1680(11)	0.2412(6)	0.0369(5)	0.075(3)
C3	0.1396(10)	0.2581(6)	0.1174(5)	0.070(3)
C4	0.2749(9)	0.2586(6)	0.1594(5)	0.063(3)
C5	0.3859(9)	0.2423(6)	0.1072(5)	0.069(2)
C6	0.3835(5)	-0.0568(5)	0.1495(3)	0.039(2)
C7	0.4914(6)	-0.0268(5)	0.2144(3)	0.043(2)
C8	0.6383(7)	-0.0635(7)	0.2111(4)	0.062(2)
C9	0.7391(10)	-0.0287(10)	0.2724(5)	0.084(3)
C10	0.6946(9)	0.0365(8)	0.3365(4)	0.079(3)
C11	0.5498(9)	0.0693(7)	0.3419(4)	0.071(3)
C12	0.4482(8)	0.0390(6)	0.2803(3)	0.052(2)
C13	0.3764(6)	-0.1829(5)	0.1171(3)	0.042(2)
C14	0.4311(6)	-0.2943(5)	0.1535(4)	0.046(2)
C15	0.4042(7)	-0.4105(5)	0.1182(4)	0.057(2)
C16	0.3248(8)	-0.4165(6)	0.0462(4)	0.061(2)
C17	0.2762(7)	-0.3086(6)	0.0075(4)	0.057(2)
C18	0.3046(6)	-0.1906(5)	0.0416(3)	0.044(2)
C19	0.2649(8)	-0.0665(6)	0.0060(3)	0.051(2)
C20	0.0899(7)	-0.0356(5)	0.1276(4)	0.052(2)

<sup>a</sup> For anisotropic atoms, the  $U$  value is  $U_{eq}$ , calculated as  $U_{eq} = 1/3 \sum_i \sum_j U_{ij} a_i^* a_j^* A_{ij}$  where  $A_{ij}$  is the dot product of the  $i$ th and  $j$ th direct space unit cell vectors.

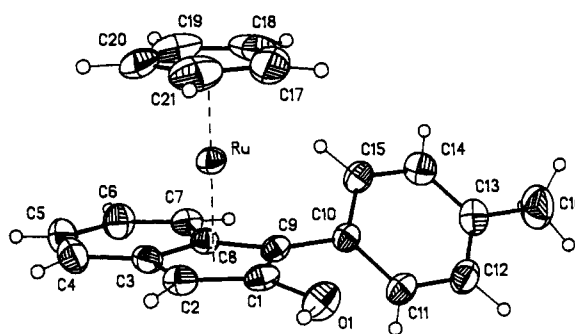


Figure 5. Structure and labeling scheme for 11b with 50% probability thermal ellipsoids.

about the length of a normal  $sp^2$ - $sp^2$  single bond (1.48 Å).<sup>12</sup> The torsion angle of C18-C13-C6-Ru is 18.4°. The dihedral angle between Ru-C6-C13 and C8-C7-C12 is 46.2°.

Complexes 5 were prepared to explore carbene migratory insertions. We were therefore surprised when, instead of undergoing insertion which, as mentioned above, could be readily detected by isomerization to the 1-metallaindene, they rearranged quantitatively to 11 when warmed to 50 °C overnight or when simply allowed to remain in solution at room temperature for a few days. These products showed neither CO absorptions in the IR nor typical carbene-carbon resonance in the <sup>13</sup>C NMR. In their <sup>1</sup>H NMR, in addition to aromatic resonances they showed new Cp signals (e.g. at δ 4.10 ppm for 11a), singlets around δ 5.3 ppm (e.g. δ 5.28 ppm for 11a), and a broad peak at about δ 3 ppm (e.g. δ 2.90 ppm for 11a) with an intensity ratio of 5:1:1. As expected of a hydroxyl group, the last peak disappeared upon addition of D<sub>2</sub>O. The proposed ruthenocene structures 11 were confirmed by X-ray structural analysis of 11b.

An ORTEP view of 11b is shown in Figure 5. Selected bond distances and angles are listed in Table 5, and positional parameters are given in Table 6. The Cp ring and the indenyl ring are parallel with a dihedral angle of

**Table 5. Selected Bond Lengths (Å) and Angles (deg) for 11b**

Bond Lengths			
Ru-C(1)	2.220(4)	Ru-C(2)	2.181(5)
Ru-C(3)	2.204(4)	Ru-C(8)	2.214(4)
Ru-C(9)	2.198(4)	Ru-C(17)	2.163(8)
Ru-C(18)	2.150(10)	Ru-C(19)	2.157(6)
Ru-C(20)	2.155(6)	Ru-C(21)	2.164(6)
C(1)-O(1)	1.360(6)	C(1)-C(2)	1.426(7)
C(1)-C(9)	1.434(6)	C(2)-C(3)	1.434(6)
C(3)-C(4)	1.429(7)	C(3)-C(8)	1.436(6)
C(4)-C(5)	1.346(8)	C(5)-C(6)	1.413(8)
C(6)-C(7)	1.376(7)	C(7)-C(8)	1.432(6)
C(8)-C(9)	1.449(6)	C(9)-C(10)	1.479(6)
C(13)-C(16)	1.502(8)	C(18)-C(17)	1.437(14)
C(17)-C(21)	1.376(10)	C(18)-C(19)	1.439(14)
C(19)-C(20)	1.396(9)	C(20)-C(21)	1.385(10)
Bond Angles			
C(2)-C(1)-C(9)	110.4(4)	C(9)-C(1)-O(1)	70.2(2)
C(1)-C(2)-C(3)	106.7(4)	C(2)-C(3)-C(4)	132.3(4)
C(3)-C(8)-C(9)	108.5(4)	C(7)-C(8)-C(9)	131.7(4)
C(1)-C(9)-C(10)	126.4(4)	C(8)-C(9)-C(10)	127.7(4)
C(1)-C(9)-C(8)	105.7(4)		

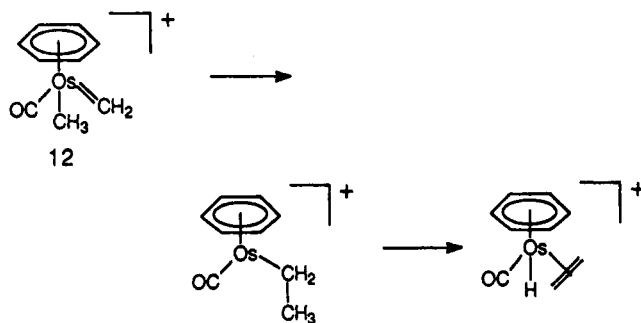
**Table 6. Fractional Coordinates and Equivalent Isotropic<sup>a</sup> Thermal Parameters (Å<sup>2</sup>) for the Non-H Atoms of Compound 11b**

atom	x	y	z	U
Ru	0.16129(4)	0.94468(3)	0.80116(2)	0.03033(8)
O1	0.2764(4)	1.1751(3)	0.7221(2)	0.0436(11)
C1	0.2967(5)	1.0981(3)	0.7831(3)	0.0308(11)
C2	0.2255(5)	1.0961(4)	0.8649(3)	0.0345(12)
C3	0.2966(5)	1.0072(4)	0.9100(3)	0.0335(12)
C4	0.2791(7)	0.9689(4)	0.9949(3)	0.045(2)
C5	0.3653(8)	0.8830(5)	1.0211(3)	0.052(2)
C6	0.4729(7)	0.8291(5)	0.9669(3)	0.048(2)
C7	0.4929(6)	0.8606(3)	0.8841(3)	0.0351(12)
C8	0.4036(5)	0.9520(4)	0.8540(3)	0.0293(10)
C9	0.3996(5)	1.0062(3)	0.7725(3)	0.0275(10)
C10	0.4928(5)	0.9794(3)	0.6961(3)	0.0301(10)
C11	0.5732(5)	1.0604(4)	0.6517(3)	0.0369(12)
C12	0.6605(7)	1.0338(4)	0.5795(3)	0.0445(14)
C13	0.6710(6)	0.9279(4)	0.5505(3)	0.0442(14)
C14	0.5913(6)	0.8480(4)	0.5955(3)	0.0429(15)
C15	0.5045(6)	0.8720(4)	0.6669(3)	0.0372(13)
C16	0.7664(10)	0.9003(6)	0.4733(4)	0.069(2)
C17	-0.0033(10)	0.9090(8)	0.7001(4)	0.084(3)
C18	0.0880(10)	0.8135(9)	0.7199(7)	0.094(4)
C19	0.0555(7)	0.7847(5)	0.8064(6)	0.063(2)
C20	-0.0536(6)	0.8613(5)	0.8358(4)	0.052(2)
C21	-0.0883(7)	0.9345(6)	0.7717(5)	0.063(2)

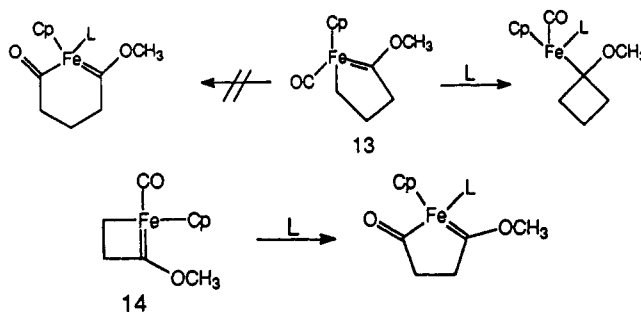
<sup>a</sup> For anisotropic atoms, the U value is  $U_{eq}$ , calculated as  $U_{eq} = \frac{1}{3} \sum_i \sum_j U_{ij} a_i^* a_j^*$  where  $A_i \cdot A_j$  is the dot product of the *i*th and *j*th direct space unit cell vectors.

0.3(3)°. The phenyl ring is not conjugated with the indenyl ring; the dihedral angle between these two rings is 45.6-(2)°. The average bond distances of Ru-Cp and Ru-indenyl (five membered ring carbons) are 2.158(4) and 2.2034(4) Å, respectively.

A reasonable mechanism for the formation of 11 from 5 is given in Scheme 2. In this mechanism the five membered ring first expands to an acyl complex (6) which then contracts to a new five membered ring. The ring expansion is interesting because it is an example of preferential carbonyl migratory insertion over carbene insertion which is counter to what appears (from very limited examples) to be the norm. For example, Werner<sup>18</sup> found only carbene insertion in 12 and we found a similar result in the cyclic carbene 13 which gave only carbene insertion despite the attendant cyclobutane strain.<sup>4</sup> On



the other hand, with enough bias as in 14<sup>5</sup> and, presumably



in 5 (due to ring strain in benzocyclobutene), preferential carbonyl insertion can occur. It is not known why the thermal lability of 5a and 5b are so dramatically increased relative to their methoxy substituted precursor 3c. One possible reason is increased electrophilicity of the terminal carbonyl resulting from replacing the methoxy group with the aryl group, despite the *cis* relationship of the carbene and the carbonyl.<sup>19a</sup> Consistent with this is the shift of the carbonyl stretching frequency from 1968.3 cm<sup>-1</sup> for 5a to 1961.3 cm<sup>-1</sup> for 3c.

The conversion of 6 to 9 and/or 7 is equally interesting because it involves either an unusual carbene insertion into a metal acyl bond (for which we know of only one example)<sup>19b</sup> to give a fourteen electron intermediate (9) or initial enolization followed by insertion of the carbene into the carbon-vinyl  $\sigma$ -bond (rearrangement of the vinyl group). The latter (path a in Scheme 2) is intriguing because it leads to a sixteen electron ruthenanaphthalene 7. Attempts to trap 7 with coordinating ligands failed; for example, in the presence of PMe<sub>3</sub> at room temperature, 5a was rapidly and quantitatively converted to the adduct 8 which, upon heating to 60 °C changed from yellow to dark red [presumably due to reverting back to 5a; at 45 °C a small concentration (ca. 5%) of 5a was detected] and eventually gave 11a without showing any evidence of a PMe<sub>3</sub> adduct of 7 although a small concentration (ca. 5%) of 5a was detected. By either mechanism, the driving force for the overall reaction is clearly the stability of the metallocenes 11, a kind of product that appears to be characteristic of reactions in which transition metalla-aromatic rings may be intermediates.<sup>20</sup>

(19) (a) Berke, H.; Hoffmann, R. *J. Am. Chem. Soc.* 1978, 100, 7224. (b) Davey, C. E.; Osborn, V. A.; Winter, M. J. In *Advances in Metal Carbene Chemistry*; Schubert, U. Ed.; Kluwer: Dordrecht, Boston, London, 1988; p 159.

(20) For examples of metallabenzenes and derivatives, see: (a) reference 8. (b) Elliott, G. P.; Roper, W. R.; Waters, J. M. *J. Chem. Soc., Chem. Commun.* 1982, 811. (c) Bleeker, J. R.; Xie, Y. F.; Peng, W. J.; Chiang, M. *J. Am. Chem. Soc.* 1989, 111, 4118. (d) Bleeker, J. R.; Peng, W. J.; Xie, Y. F.; Chiang, M. *J. Organometallics* 1990, 9, 1113. (e) Bleeker, J. R.; Xie, Y. F.; Bass, L.; Chiang, M. *J. Am. Chem. Soc.* 1991, 113, 4703. (f) Bleeker, J. R. *Acc. Chem. Res.* 1991, 24, 271. (g) Bleeker, J. R.; Bass, L. A.; Xie, Y. F.; Chiang, M. *J. Am. Chem. Soc.* 1992, 114, 4213.

### Experimental Section

All experiments involving organometallic compounds were carried out under nitrogen using Schlenk, vacuum line, and glovebox techniques. THF, diethyl ether, and toluene were distilled from sodium benzophenone ketyl. Hexane was distilled from  $\text{CaH}_2$ .  $\text{CpM}(\text{CO})_3\text{Na}$  ( $M = \text{Mo}, \text{W}$ )<sup>21</sup> and  $\text{CpRu}(\text{CO})_2\text{Na}$ <sup>22</sup> were prepared as previously described. 2-Bromobenzyl bromide,  $n\text{-BuLi}$ ,  $\text{Me}_3\text{OBF}_4$ , and  $\text{PMe}_3$  were purchased from Aldrich Co. and used as received.  $\text{Me}_3\text{SiSO}_3\text{CF}_3$  was purchased from Aldrich Co. and was distilled by vacuum transfer over a proton sponge prior to use.  $\text{H}_2\text{O}$  was degassed by bubbling  $\text{N}_2$  through it for a few hours. Silica gel was degassed under vacuum for 5 h. NMR spectra were recorded on a VAX-300 with TMS or solvent peaks as references. IR spectra were obtained on a Perkin-Elmer 1600 FTIR. Mass spectra were carried out on a Finnigan Mat 95Q. Elemental analyses were performed in the microanalysis lab in the Chemistry Department at the University of Florida. Melting points were measured in the sealed capillaries and were not corrected.

**Preparation of  $\text{CpMo}(\text{CO})_3\text{CH}_2\text{-o-BrC}_6\text{H}_4$ , 2a.** To a solution of  $\text{CpMo}(\text{CO})_3\text{Na}$  prepared from 5.8 g of  $\text{Mo}(\text{CO})_6$  (23 mmol) and  $\text{CpNa}$  in 50 mL of THF was added 5.5 g (22 mmol) of 2-bromobenzyl bromide at  $-30^\circ\text{C}$ . The mixture was warmed to room temperature in 0.5 h and stirred for another 3 h. The solvent was evaporated to dryness and the residue extracted three times with 300 mL of hexane. The combined extracts were concentrated to 100 mL at  $0^\circ\text{C}$  to give 3.3 g of orange crystals. The mother liquor was concentrated to 50 mL and kept at  $-30^\circ\text{C}$  overnight to give a second crop of 1.0 g (yield, 51%), mp  $97\text{--}100^\circ\text{C}$ . IR (hexane solution): 2022.2, 1948.8, 1936.4  $\text{cm}^{-1}$ .  $^1\text{H}$  NMR ( $\text{C}_6\text{D}_6$ ):  $\delta$  7.40 (m, 2H), 6.90 (m, 1H), 6.57 (m, 1H), 4.48 (s, 5H), 2.91 (s, 2H).  $^{13}\text{C}$  NMR ( $\text{C}_6\text{D}_6$ ):  $\delta$  228.9, 151.95, 132.77, 129.39, 125.11, 123.23, 2.95. Anal. Calcd for  $\text{C}_{15}\text{H}_{11}\text{BrO}_3\text{Mo}$ : C, 43.40; H, 2.67. Found: C, 43.50; H, 2.90.

**Preparation of  $\text{CpW}(\text{CO})_3\text{CH}_2\text{-o-BrC}_6\text{H}_4$ , 2b.** Similar to the preparation of 2a, 4.0 g of 2-bromobenzyl bromide reacted with  $\text{CpW}(\text{CO})_3\text{Na}$  prepared from 5 g of  $\text{W}(\text{CO})_6$ . After the solvent was evaporated, the reaction mixture was extracted with a mixture of toluene and hexane (1/3, v/v). The resulting yellow solution was kept at  $-50^\circ\text{C}$  for 5 h to give 3.8 g (yield 52%) of orange crystals, mp  $125\text{--}128^\circ\text{C}$ . IR (hexane solution): 2021.0, 1938.7, 1928.8  $\text{cm}^{-1}$ .  $^1\text{H}$  NMR ( $\text{C}_6\text{D}_6$ ):  $\delta$  7.45 (m, 1H), 7.35 (m, 1H), 6.90 (m, 1H), 6.55 (m, 1H), 4.50 (s, 5H), 2.97 (s, 2H).  $^{13}\text{C}$  NMR ( $\text{C}_6\text{D}_6$ ):  $\delta$  219.12, 152.33, 132.65, 129.37, 125.14, 123.13, 91.94,  $-8.91$ . Anal. Calcd for  $\text{C}_{15}\text{H}_{11}\text{BrO}_3\text{W}$ : C, 35.82; H, 2.20. Found: C, 35.63; H, 2.15.

**Preparation of  $\text{CpRu}(\text{CO})_2\text{CH}_2\text{-o-BrC}_6\text{H}_4$ , 2c.** To a solution of  $\text{CpRu}(\text{CO})_2\text{Na}$  prepared from 2.2 g (4.95 mmol) of  $[\text{CpRu}(\text{CO})_2]_2$  and amalgam in 300 mL of THF was added 2.48 g of 2-bromobenzyl bromide at  $-78^\circ\text{C}$ . The mixture was warmed to room temperature slowly and stirred overnight. The solvent was removed under a vacuum and the residue was chromatographed on a silica gel column ( $2 \times 20$  cm) with hexane. The solution was collected until the colored impurity came out. The solvent was concentrated to 20 mL, and the solution was kept at  $-20^\circ\text{C}$  overnight to give 2.56 g (yield 66%) of 2c as white crystals, mp  $52\text{--}53^\circ\text{C}$ . IR (hexane solution): 2025.1, 1989.0  $\text{cm}^{-1}$ .  $^1\text{H}$  NMR ( $\text{C}_6\text{D}_6$ ):  $\delta$  7.50 (d, 1H), 7.28 (d, 1H), 6.98 (t, 1H), 6.60 (t, 1H), 4.46 (s, 5H), 3.03 (s, 2H).  $^{13}\text{C}$  NMR ( $\text{C}_6\text{D}_6$ ):  $\delta$  210.00, 154–121 (phenyl), 88.39, 33.32. Anal. Calcd for  $\text{C}_{14}\text{H}_{11}\text{O}_2\text{BrRu}$ : C, 42.86; H, 2.81. Found: C, 42.87; H, 2.80.

**Preparation of Metallaindene 3a ( $M = \text{Mo}$ ).** To a solution of 0.30 g (0.72 mmol) of 2a in 25 mL of THF at  $-100^\circ\text{C}$  was added 1.1 mmol of  $n\text{-BuLi}$ /diethyl ether solution by syringe over 5 min. The color of the solution changed from yellow to deep red. The mixture was warmed to room temperature in a few hours and stirred overnight. The deep red reaction mixture was cooled to  $-20^\circ\text{C}$ , and 0.2 g of  $\text{Me}_3\text{OBF}_4$  was added in a few portions over

20 min. The reaction mixture was stirred for an additional 1 h at  $-20^\circ\text{C}$  with warming to  $0^\circ\text{C}$ . The excess of  $\text{Me}_3\text{OBF}_4$  was quenched with 30 mL of water. The reaction mixture was extracted two times with 100 mL of hexane. The solvent was evaporated and the residue was chromatographed on a silica gel column ( $2 \times 20$  cm) using diethyl ether/hexane (1/20, v/v) as solvent. The red brown band was collected, and the solvent was evaporated to dryness. The residue was dissolved in 2 mL of toluene, and then 30 mL of hexane was added. The solution was kept at  $-78^\circ\text{C}$  for a few days to give 82 mg (32.5%) of brown red crystals. IR (hexane solution): 1958.3, 1895.1  $\text{cm}^{-1}$ .  $^1\text{H}$  NMR ( $\text{C}_6\text{D}_6$ ):  $\delta$  7.60 (m, 1H), 7.43 (m, 1H), 7.06 (m, 1H), 6.85 (m, 1H), 4.74 (s, 5H), 3.98 (m, 3H), 3.36 (d, 1H,  $^2J_{\text{HH}} = 12.7$  Hz), 2.87 (d, 1H,  $^2J_{\text{HH}} = 12.7$  Hz). Anal. Calcd for  $\text{C}_{16}\text{H}_{14}\text{O}_3\text{Mo}$ : C, 54.88; H, 4.03. Found: C, 54.56; H, 4.28.

**Preparation of Metallaindene 3b ( $M = \text{W}$ ).** Similar to the preparation of 3a, 0.3 g (0.60 mmol) of 2b was treated with 1.0 mmol of  $n\text{-BuLi}$  at  $-100^\circ\text{C}$  in THF. The reaction mixture was stirred overnight and treated with 0.25 g of  $\text{Me}_3\text{OBF}_4$ . The excess of methylating reagent was destroyed by water and the mixture extracted with hexane. The solvent was evaporated, and the residue was chromatographed twice on a silica gel column ( $2 \times 25$  cm) with a hexane/diethyl ether (20/1, v/v) mixture as solvent. The brown-red band was collected to give a deep red solution. The solvent was evaporated, and the residue was recrystallized from toluene/hexane mixture to give 0.12 g (46%) of dark-red crystals, mp  $140\text{--}151^\circ\text{C}$  dec. IR (hexane solution): 1956.4, 1987.8  $\text{cm}^{-1}$ .  $^1\text{H}$  NMR (at room temperature in  $\text{CDCl}_3$ ):  $\delta$  7.08 (m, 1H), 6.95 (m, 1H), 6.85 (m, 1H), 6.60 (m, 1H), 5.21 (s, 5H), 4.17 (s, 3H), 2.84 (d, 1H,  $^2J_{\text{HH}} = 14.2$  Hz), 2.46 (d, 1H,  $^2J_{\text{HH}} = 14.2$  Hz).  $^{13}\text{C}$  NMR ( $\text{C}_6\text{D}_6$ ):  $\delta$  294.18, 235.86, 225.37, 166.00, 137.56, 130.38, 127.24, 124.05, 119.95, 91.46, 64.55, 16.71. Anal. Calcd for  $\text{C}_{16}\text{H}_{14}\text{O}_3\text{W}$ : C, 43.86; H, 3.22. Found: C, 43.80; H, 3.27.

$^{13}\text{C}$ -enriched 3b (enriched for CO and carbene carbon) was prepared similarly from  $\text{W}(\text{CO})_4(^{13}\text{CO})_2$ .

**Preparation of Metallaindene 3c ( $M = \text{Ru}$ ).** To a solution of 0.30 g (0.76 mmol) of 2c in 20 mL of THF was added 1.2 equiv of  $n\text{-BuLi}$  pentane solution at  $-100^\circ\text{C}$ . The solution was stirred overnight while the mixture was allowed to warm to room temperature slowly. The solution was then cooled to  $-30^\circ\text{C}$ , and  $\text{Me}_3\text{OBF}_4$  was added in small portions until the pH reached 6–7 (about 0.3 g is needed). The orange color of the solution changed to reddish at ca.  $0^\circ\text{C}$  within 30 min, and the excess of  $\text{Me}_3\text{OBF}_4$  was destroyed with 20 mL of water. The mixture was extracted with hexane three times, and the combined extracts were evaporated to dryness. The residue was chromatographed on a silica gel column with hexane, and the red band was collected. After most of the solvent had been removed, the solution was kept at  $-10^\circ\text{C}$  for 5 h to give 110 mg (44%) of red crystals, mp  $110\text{--}111^\circ\text{C}$ . IR (hexane solution): 1961.3  $\text{cm}^{-1}$ .  $^1\text{H}$  NMR ( $\text{CDCl}_3$ ):  $\delta$  7.0–7.6 (m, 4H), 5.23 (s, 5H), 4.51 (s, 3H), 3.18 (d, 1H,  $^2J_{\text{HH}} = 13.9$  Hz), 3.05 (d, 1H,  $^2J_{\text{HH}} = 13.9$  Hz).  $^{13}\text{C}$  NMR ( $\text{CDCl}_3$ ):  $\delta$  294.16, 206.07, 167.55, 152.34, 131.30, 127.38, 123.70, 118.99, 86.80, 67.00, 10.27. HRMS (EI,  $m/e$ ): calcd for ( $M^+$ ) 328.003; found 328.003. Anal. Calcd for  $\text{C}_{15}\text{H}_{14}\text{O}_2\text{Ru}$ : C, 55.05; H, 4.31. Found: C, 54.87; H, 4.21.

**Preparation of Metallaindene 5a ( $M = \text{Ru}, \text{Ar} = \text{Ph}$ ).** To a red solution of 150 mg (0.457 mmol) of 2c in 30 mL of THF was added at  $-78^\circ\text{C}$  a solution of 0.54 mmol of  $\text{PhLi}$  solution in diethyl ether by syringe over 10 min. The color of the solution changed to dark brown-reddish as the bath temperature warmed to  $-25^\circ\text{C}$  in 4 h. To this solution was added 2 equiv of trimethylsilyl triflate at  $-196^\circ\text{C}$  by vacuum line transfer. A dark red color was produced when the temperature was allowed to increase from  $-196^\circ\text{C}$  to room temperature over a period of 1 h. Removing the THF under vacuum led to a black-purple residue which was chromatographed on a silica gel column with hexane as solvent. The black-purple band was collected, and the concentrated solution was cooled to  $-30^\circ\text{C}$  overnight to give 110 mg (yield, 65%) of black-red crystals, mp  $114\text{--}115^\circ\text{C}$ . IR (hexane solution): 1968.3  $\text{cm}^{-1}$ .  $^1\text{H}$  NMR ( $\text{C}_6\text{D}_6$ ):  $\delta$  6.7–7.4 (m, 9H), 4.87 (s, 5H), 3.72 (d, 1H,  $^2J_{\text{HH}} = 12.6$  Hz), 2.58 (d, 1H,  $^2J_{\text{HH}}$

(21) Piper, T. W.; Wilkinson, G. *Inorg. Nucl. Chem.* 1956, 3, 104.

(22) Blackmore, T.; Bruce, M. I.; Stone, F. G. A. *J. Chem. Soc. A* 1968, 2158.

Table 7. Crystallographic Data

	3b	5a	11b
A. Crystal Data (298 K)			
<i>a</i> , Å	9.945(2)	9.082(1)	8.452(1)
<i>b</i> , Å	13.207(2)	10.601(1)	12.258(1)
<i>c</i> , Å	11.304(2)	16.827(2)	15.812(2)
$\alpha$ , deg	90	90	90
$\beta$ , deg	107.38(2)	92.57(1)	90
$\gamma$ , deg	90	90	90
<i>V</i> , Å <sup>3</sup>	1416.9(5)	1618.4(3)	1638.2(3)
<i>d</i> <sub>calc</sub> , g cm <sup>-3</sup>	2.054	1.532	1.571
empirical formula	C <sub>16</sub> H <sub>14</sub> O <sub>3</sub> W	C <sub>20</sub> H <sub>16</sub> ORu	C <sub>21</sub> H <sub>18</sub> ORu
<i>f</i> <sub>w</sub>	438.12	373.40	387.42
cryst syst	monoclinic	monoclinic	orthorhombic
space group	<i>P</i> 2 <sub>1</sub> / <i>n</i>	<i>P</i> 2 <sub>1</sub> / <i>n</i>	<i>P</i> 2 <sub>1</sub> 2 <sub>1</sub> 2 <sub>1</sub>
<i>Z</i>	4	4	4
<i>F</i> (000), electrons	832	752	784
cryst size (mm <sup>3</sup> )	0.42 × 0.15 × 0.05	0.34 × 0.23 × 0.15	0.39 × 0.31 × 0.14
B. Data Collection (298 K)			
radiation/ $\lambda$ , Å	Mo K $\alpha$ /0.710 73	Mo K $\alpha$ /0.710 73	Mo K $\alpha$ /0.710 73
mode	$\omega$ -scan	$\omega$ -scan	$\omega$ -scan
scan range	symmetrically over $X^\circ$ about K $\alpha$ <sub>1,2</sub> maximum ( $X = 1.5, 1.2, \& 1.2$ for 1–3, respectively)		
background	offset 1.0 and –1.0 in $\omega$ from K $\alpha$ <sub>1,2</sub> maximum		
scan rate, deg min <sup>-1</sup>	3–6	3–6	3–6
2 $\theta$ range, deg	3–55	3–55	3–60
range of <i>hkl</i>	0 ≤ <i>h</i> ≤ 12 0 ≤ <i>k</i> ≤ 17 –14 ≤ <i>l</i> ≤ 14	0 ≤ <i>h</i> ≤ 11 0 ≤ <i>k</i> ≤ 13 –21 ≤ <i>l</i> ≤ 21	0 ≤ <i>h</i> ≤ 22 0 ≤ <i>k</i> ≤ 17 0 ≤ <i>l</i> ≤ 22
total no. of reflns measd	3613	4175	2741
no. of unique reflns	3273	3730	2716
abs coeff $\mu$ (Mo K $\alpha$ ), mm <sup>-1</sup>	8.16	9.7	9.6
min/max transm	0.317/0.694	0.789/0.868	0.723/0.828
C. Structure Refinement <sup>a</sup>			
<i>S</i> , goodness-of-fit	1.52	1.96	1.34
no. of reflns used, <i>I</i> > 2 $\sigma$ ( <i>I</i> )	2295	2851	2451
no. of variables	217	263	261
<i>R</i> <sub>w</sub> , %	3.95/4.56	4.57/6.10	3.38/3.93
<i>R</i> <sub>int</sub> , %	1.69	1.84	0
max shift/esd	0.001	0.003	0.006
min peak in diff Fourier map, e Å <sup>-3</sup>	–2.0	–0.59	–0.38
max peak in diff Fourier map, e Å <sup>-3</sup>	2.6	1.03	0.43

<sup>a</sup> Relevant expressions are as follows, where  $F_o$  and  $F_c$  represent respectively the observed and calculated structure factor amplitudes. Function minimized was  $w(|F_o| - |F_c|)^2$ , where  $w = (\sigma(F))^{-2}$ .  $R = \sum(|F_o| - |F_c|)/\sum|F_o|$ .  $R_w = [\sum w(|F_o| - |F_c|)^2/\sum|F_o|^2]^{1/2}$ .  $S = [\sum w(|F_o| - |F_c|)^2/(m - n)]^{1/2}$ .

= 12.6 Hz). <sup>13</sup>C NMR (C<sub>6</sub>D<sub>6</sub>):  $\delta$  309.53, 209.77, 166.96, 160.29, 158.12, 131.09, 129.14, 128.53, 127.79, 124.46, 122.46, 122.78, 90.32, 15.87. MS (EI, *m/e*): 374 (M<sup>+</sup>). Anal. Calcd for C<sub>20</sub>H<sub>16</sub>ORu: C, 64.35; H, 4.32. Found: C, 64.29; H, 4.28.

**Preparation of Metallindene 5b (Ar = *p*-CH<sub>3</sub>C<sub>6</sub>H<sub>4</sub>).** Similar to the preparation of complex 5a, 150 mg of 3c was reacted with *p*-tolyllithium and subsequent treatment with Me<sub>3</sub>SiSO<sub>3</sub>-CF<sub>3</sub> gave 5b as black crystals in 58% yield, mp 95–96 °C. IR (hexane solution): 1966.7 cm<sup>-1</sup>. <sup>1</sup>H NMR (C<sub>6</sub>D<sub>6</sub>):  $\delta$  6.8–7.6 (m, 8H), 4.91 (s, 5H), 3.73 (d, 1H, <sup>2</sup>*J*<sub>HH</sub> = 12.6 Hz), 2.63 (d, 1H, <sup>2</sup>*J*<sub>HH</sub> = 12.6 Hz), 2.10 (s, 3H). <sup>13</sup>C NMR (C<sub>6</sub>D<sub>6</sub>):  $\delta$  309.16, 209.90, 166.84, 160.32, 156.00, 139.56, 131.05, 128.13, 124.40, 122.84, 90.20, 21.40, 15.60. MS (EI, *m/e*): 388 (M + 1). Anal. Calcd for C<sub>21</sub>H<sub>18</sub>ORu: C, 65.10; H, 4.65. Found: C, 65.09; H, 4.68.

**Thermolysis of 5a—Preparation of Ruthenocene 11a.** A dark solution of 30 mg of 5a in 2 mL of C<sub>6</sub>D<sub>6</sub> in a sealed NMR tube was heated at 50 °C for 12 h to give an orange solution. The reaction was monitored by NMR, and the transformation from 5a to 11a was complete when an orange solution was observed. The same results can be obtained if the solution of 5a was allowed to sit at room temperature for about 5 days. The solvent was evaporated under vacuum to give 30 mg (100%) of an orange solid, mp 120–135 °C dec. <sup>1</sup>H NMR (C<sub>6</sub>D<sub>6</sub>):  $\delta$  6.75–7.8 (m, 9H), 5.28 (s, 1H), 4.10 (s, 5H), 2.90 (br, 1H). <sup>13</sup>C NMR (C<sub>6</sub>D<sub>6</sub>): 135.7, 131.2, 128.7, 127.1, 126.9, 126.1, 123.8, 123.0, 122.9, 90.3, 88.4, 56.7, 31.8. MS (EI, *m/e*): 374 (M<sup>+</sup>). Anal. Calcd for C<sub>20</sub>H<sub>16</sub>ORu: C, 64.35; H, 4.32. Found: C, 64.16; H, 4.31.

**Thermolysis of 5b—Preparation of Ruthenocene 11b.** The method used was the same as that for the preparation of 11a,

except the temperature used was 70 °C. 11b was formed quantitatively. <sup>1</sup>H NMR (C<sub>6</sub>D<sub>6</sub>):  $\delta$  6.75–7.74 (m, 8H), 5.33 (s, 1H), 4.15 (s, 5H), 2.80 (br, 1H), 2.20 (s, 3H). <sup>13</sup>C NMR (C<sub>6</sub>D<sub>6</sub>):  $\delta$  136.64–122.84 (aromatic carbon), 88.40, 86.68, 77.83, 71.78, 56.56, 21.20. Anal. Calcd for C<sub>21</sub>H<sub>18</sub>ORu: C, 65.10; H, 4.65. Found: C, 65.09; H, 4.68.

**Preparation of 8.** To a solution of 20 mg (0.54 mmol) of 5a in 2 mL of C<sub>6</sub>D<sub>6</sub> was added 20  $\mu$ L of PMe<sub>3</sub> at room temperature. A color change of the solution from dark red to orange occurred immediately. The <sup>1</sup>H NMR showed the PMe<sub>3</sub> has added to 5a to form 8 completely. The solvent was evaporated to give 23 mg (100%) of an orange solid. <sup>1</sup>H NMR (C<sub>6</sub>D<sub>6</sub>):  $\delta$  6.6–7.6 (m, 9H), 4.33 (s, 5H), 3.89 (dd, 1H, <sup>2</sup>*J*<sub>HH</sub> = 14.8 Hz, <sup>4</sup>*J*<sub>PH</sub> = 3.8 Hz), 2.91 (dd, 1H, <sup>2</sup>*J*<sub>HH</sub> = 14.8 Hz, <sup>4</sup>*J*<sub>PH</sub> = 3.8 Hz), 0.9 (br, 9H). This broad peak at 0.9 ppm (PMe<sub>3</sub>) appeared as three groups of doublets at –78 °C at 1.55, 0.58, and 0.49 ppm with coupling constants <sup>2</sup>*J*<sub>PH</sub> = 9.6, 11.9, and 9.0 Hz, respectively. Two groups of doublets were observed at –40 °C at 1.68 and 0.62 ppm with an intensity ratio of 1:2. The two groups of doublets coalesced at room temperature to give a broad peak. <sup>13</sup>C NMR (C<sub>6</sub>D<sub>6</sub>):  $\delta$  211.95 (d, <sup>2</sup>*J*<sub>PC</sub> = 5.5 Hz), 162.61, 155.98, 146.99, 130.63, 129.28, 129.20, 127.83, 126.12 (d, *J* = 3.2 Hz), 125.8 (br), 123.84, 121.87, 87.26, 4.63. MS (EI, *m/e*): 374 (M<sup>+</sup>). Anal. Calcd for C<sub>23</sub>H<sub>26</sub>OPRu: C, 61.48; H, 5.56. Found: C, 61.04; H, 5.58.

**Crystallographic Analysis.** Crystal data and numerical details of the structure determinations are given in Table 7. The black-red single crystals of 3b were obtained from a toluene/hexane solution at –10 °C. Black-red crystals of 5a were grown from hexane by slowly cooling to –78 °C. Orange crystals of 11b

were grown from benzene solution at room temperature. All crystals used in diffraction intensity measurements were mounted in thin-walled glass capillaries. Data were collected at room temperature on a Siemens R3m/V diffractometer equipped with a graphite monochromator utilizing Mo K $\alpha$  radiation ( $\lambda = 0.71073$  Å). A total of 50 reflections with  $20.0^\circ \leq 2\theta \leq 22.0^\circ$  were used to refine the cell parameters. Totals of 3613, 4175, and 2741 reflections, for **3b**, **5a**, and **11b**, respectively, were collected using the  $\omega$ -scan method (1.2° scan range and 3–6° min<sup>-1</sup> scan speed depending on the intensity). Four reflections ( $\bar{1}\bar{1}0$ ,  $\bar{1}\bar{1}2$ ,  $1\bar{2}0$ ,  $1\bar{2}\bar{2}$ ), ( $2\bar{2}\bar{3}$ ,  $120$ ,  $023$ ,  $202$ ), and ( $2\bar{2}1$ ,  $023$ ,  $2\bar{2}1$ ,  $0\bar{1}\bar{3}$ ) for **3b**, **5a**, and **11b**, respectively, were measured every 96 reflections to monitor the instrument and crystal stability (maximum correction on  $I$  was <1%). Absorption corrections were applied on the basis of measured crystal faces using *SHELXTL plus*. Absorption coefficients: **3b**,  $\mu = 8.16$  mm<sup>-1</sup> (min and max transmission factors are 0.317 and 0.694, respectively); **5a**,  $\mu = 9.7$  mm<sup>-1</sup> (min and max transmission factors are 0.789 and 0.868, respectively); **11b**,  $\mu = 9.6$  mm<sup>-1</sup> (min and max transmission factors are 0.723 and 0.828, respectively).

The structures were solved by the heavy atom method in *SHELXTL plus*<sup>23</sup> from which the positions of the W atom in **3b** and the Ru atoms in **5a** and **11b** were obtained. The rest of the non-H atoms were obtained from subsequent difference Fourier maps. The structures were refined in *SHELXTL plus* using full-matrix least squares. All of the non-H atoms were refined with anisotropic thermal parameters. The non-H atoms were treated anisotropically. The methyl H atoms and those of C8 in **3b** were calculated in idealized positions, and their thermal parameters were fixed at 0.08. The rest of the H atoms were located from a difference Fourier map and were refined without any constraints. In **5a** the H atoms were located from a difference Fourier map and were refined without any constraints. In **11b**,

(23) Sheldrick, G. M. *SHELXTL plus*; Nicolet XRD Corp.: Madison, WI, 1990.

they were located from a difference Fourier map and refined freely; except for the C16 hydrogen atoms which were calculated in idealized positions and their thermal parameters were fixed at 0.08. A total of 217, 263, and 261 parameters for **3b**, **5a**, and **11b**, respectively, were refined and  $\sum w(|F_o| - |F_c|)^2$  was minimized;  $w = 1/(\sigma(F_o))^2$ ,  $s(F_o) = 0.5kI^{-1/2}\{[s(I)]^2 + (0.02I)^2\}^{1/2}$ ,  $I$  (intensity) =  $(I_{\text{peak}} - I_{\text{background}})(\text{scan rate})$ , and  $\sigma(I) = (I_{\text{peak}} + I_{\text{background}})^{1/2}(\text{scan rate})$ ,  $k$  is the correction due to decay and  $Lp$  effects and 0.02 is a factor used to down weight intense reflections and to account for instrument instability.  $R = 0.0395$  and  $R_w = 0.0456$  for **3b**,  $R = 0.0457$  and  $R_w = 0.061$  for **5a**, and  $R = 0.0338$  and  $R_w = 0.0393$  for **11b** in the last cycle of refinement. The linear absorption coefficient was calculated from values in ref 24. Scattering factors for non-hydrogen atoms were taken from Cromer and Mann<sup>26</sup> with anomalous dispersion corrections from Cromer and Liberman,<sup>26</sup> while those of hydrogen atoms were from Stewart, Davidson, and Simpson.<sup>27</sup>

**Acknowledgment.** The authors gratefully acknowledge support of this research from the National Science Foundation, the University of Florida Division of Sponsored Research, and the Chevron Research and Technology Co.

**Supplementary Material Available:** X-ray data for **3b**, **5a**, and **11b** including tables of bond lengths and angles, thermal parameters, and atomic coordinates (14 pages). Ordering information is given on any current masthead page.

OM930706K

(24) *International Tables for X-ray Crystallography*; Kynoch Press: Birmingham, U. K. (Present distributor: D. Reidel, Dordrecht), 1974; Vol. IV, p 55.

(25) Cromer, D. T.; Mann, J. B. *Acta Crystallogr.* 1968, *A24*, 321.

(26) Cromer, D. T.; Liberman, D. *J. Chem. Phys.* 1970, *53*, 1891.

(27) Stewart, R. F.; Davidson, E. R.; Simpson, W. T. *J. Chem. Phys.* 1965, *42*, 3175.